IEEE Access
Multidisciplinary | Rapid Review | Open Access Journal

Received December 1, 2020, accepted December 24, 2020, date of publication December 31, 2020,
date of current version January 13, 2021.

Digital Object Identifier 10.1109/ACCESS.2020.3048645

Instrumented Ergonomic Risk Assessment Using Wearable Inertial Measurement Units: Impact of Joint Angle Convention

AHMED HUMADI, MILAD NAZARAHARI, RAFIQ AHMAD, AND HOSSEIN ROUHANI, (Member, IEEE)
Department of Mechanical Engineering, University of Alberta, Edmonton, AB T6G 1H9, Canada

Corresponding author: Hossein Rouhani (hrouhani@ualberta.ca)

This work was supported in part by the Alberta Ministry of Labour, Occupational Health and Safety (OHS) Futures–Research Funding Program, under Grant OHSFRFPP 095245031, and in part by the Hadhramout Establishment for Human Development Scholarship.

ABSTRACT The Rapid Upper Limb Assessment (RULA) is frequently used to monitor body posture for early risk prevention of work-related musculoskeletal disorders. However, RULA measurements that are based on workers' self-report or external rater observation suffer from low repeatability. Thus, the objective of this study was to investigate the accuracy and repeatability of an inertial measurement unit (IMU) system for in-field RULA score assessment during manual material handling tasks using 3D Cardan angles and 2D projection angles against reference values obtained by a motion-capture camera system. The experimental results showed that for trunk and neck joint angles, the 2D convention had significantly ($p<0.05$) smaller root-mean-square error (RMSE), while for other upper-body angles, the convention with significantly smaller RMSE depended on the angle under analysis. Also, the 3D convention showed a ''moderate'' agreement with the reference system, while the 2D convention showed a ''substantial'' agreement for two tasks and a ''moderate'' agreement for one task. Moreover, the intraclass correlation coefficients ranged from 0.82 to 0.94 for the 3D convention and 0.87 to 0.95 for the 2D convention for repeated trials performed by each participant. Therefore, the wearable IMU system, along with the 2D convention, could be considered as an accurate and repeatable ergonomic risk assessment tool.

INDEX TERMS Ergonomic risk assessment, inertial measurement unit, material handling tasks, RULA, work-related musculoskeletal disorders.

I. INTRODUCTION

The physical factors such as forces exerted on the musculoskeletal system, postures adopted, or work cycles contribute to the development or progression of work-related musculoskeletal disorders (WMDs) such as tendon inflammations, nerve compression disorders, osteoarthrosis, myalgia, and low back pain [1], [2]. WMDs account for a major cause of nonfatal occupational injuries [3]. These disorders have severe consequences for the workforce and impose a significant financial burden on healthcare systems [4].

Therefore, several assessment methods have been proposed to assess the human body motion and posture during task execution to characterize and mitigate these physical factors towards reducing the risk of injury. These assessment methods are grouped by their way of workplace observation into three groups, including self-report, observational, and direct methods [5]. The self-reporting methods are in the form of questionnaires [6], checklists [7], or interviews [8], and depend on the subjective report of the individuals about their behaviour, symptoms, and attitude. Despite being easy to measure and low cost of implementation for real-world applications, subjective reporting could lead to an inaccurate perception of the WMDs factors exposure among workers [9].

The observational methods are classified into simple and advanced methods [10]. Simple observational methods record the worker postures in pre-designed proforma sheets by an independent observer. In particular, the Rapid Upper Limb Assessment (RULA) is a physical risk assessment tool that evaluates the WMDs risk factors related to the trunk, neck,

The associate editor coordinating the review of this manuscript and approving it for publication was Sabah Mohammed.

and upper-limb based on the posture's observations [11]. This method quantifies the posture risks as a single score ranging from 1 (low risk) to 7 (high risk) by applying pre-defined thresholds to segments' angular position and provides suggestions accordingly:

- Scores 1 and 2: Acceptable posture.
- Scores 3 and 4: Further investigation, change may be needed.
- Scores 5 and 6: Further investigation, change soon.
- Score 7: Investigate and implement change.

The RULA scores should be monitored continuously during the whole work/activity duration to identify and revise the most harmful posture or longest-held posture [11]. Thus, the RULA provides quick and low-cost upper limb disorder assessment for the working population. Yet, the low inter-observer repeatability is the major shortcoming of simple observational methods [5]. Therefore, advanced observational methods based on video recording and computer analyzing, such as hands-relative-to-the-body (HARBO) [12], portable-ergonomic-observation (PEO) [13], and SIMI software (Simi Motion®) [14], were suggested to assess a variety of postures in fast-paced environments in real-time. For instance, the HARBO method was developed to record the duration of four walking posture with hands at pre-defined angular positions and a sitting posture using a hand-held personal computer [12]. Similarly, the PEO method was developed to register workers' postures and activities (the duration and number of events) at arms, neck, trunk, and knee level using a hand-held personal computer [13]. The SIMI software was also used to analyze 3D images of the workers' trunks during standard tasks involved in supermarket check-out workstations toward calculating trunk's kinematics [14]. Nevertheless, the practical functionality of these systems in real workplaces is questionable because of the self or object occlusion, limited field of view, and high operating cost [9].

Recently, the integration of direct measurement of the body posture and muscle fatigue using wearable sensing devices and observational methods for evaluating WMDs factors have been considered to increase the inter-observer repeatability and data collection accuracy [15]. Direct methods for WMDs assessment employ wearable sensing devices attached to the worker's body for direct measurement/assessment of the posture and muscle fatigue [10]. The posture measurement could be based on an inclinometer, electric goniometer, or hand-held equipment that continuously monitors the joint angles during a task [16], [17]. The muscle fatigue measurement is usually based on the readouts of an Electromyography (EMG) sensor. However, these systems were developed mainly for clinical applications rather than real workplaces. For instance, while electric goniometers are suitable for knee or elbow flexion/extension angle measurement, they cannot be used to measure trunk, shoulder, or neck angles. Also, EMG readout can be affected negatively by sweating.

On the other hand, wearable inertial measurement units (IMUs) can be used along with observational methods to evaluate the WMDs factors [18]. IMUs can measure body segments' acceleration and angular velocity, as well as kinematic parameters such as joint angles [19], [20]. Their accuracy and reliability have been validated in various applications such as gait analysis [21], daily activities monitoring [22], balance assessment [23], or ability to return to sport after knee injury [24]. Considering the advantages such as high accuracy and reliability, low cost, small size, and long battery life, IMUs can be ideal for ergonomic assessment studies.

Therefore, previous studies validated the application of IMUs along with simple observational methods for WMDs factors evaluation against human observers. For instance, Vignais *et al.* [25] used seven IMUs placed on the upper-body segments together with two goniometers to calculate joint angles and then the RULA score and provided auditory and visual feedback accordingly to decrease the hazard associated with industrial tasks. Peppoloni *et al.* [26] proposed the combination of wearable IMUs and surface EMG sensors for measuring the forearm's muscle efforts in a simulated environment to assess hazards associated with the material handling tasks. Battini *et al.* [27] proposed the application of 17 IMUs for building a biomechanical model with 20 degrees of freedom and validated the proposed system in a fashion distribution center and supermarket warehouse.

Although IMUs have been used for various biomedical applications, almost in all cases, only the accuracy and repeatability of 3D joint angles defined by the joint coordinate system (JCS) according to ISB recommendations have been validated against a reference system. At the same time, IMUs have shown great potential for applications that require the sensors to be worn for an extended period of time, while they minimally interfere with user's routines, such as ergonomic risk assessment of workers in industrial environments. However, in the application of IMUs for ergonomic risk assessment, the convention adopted for calculating the joint angles can play a significant role in RULA score calculation. In particular, JCS [28] along with the ISB recommendations for local anatomical frames [29], [30] (will be referred to as 3D joint angles hereafter), is the standard method for joint angle measurement with IMUs [20]. However, the RULA score was initially defined based on the planar projection of joint angles into anatomical planes (referred to as 2D joint angles hereafter). Notably, Manghisi *et al.* [31] showed that the RULA scores calculated using the 2D joint angles obtained by Kinect V2 had a ''perfect'' proportion agreement with those obtained by the gold-standard camera-based system. The IMUs, unlike Kinect V2, can calculate joint angles using both 2D and 3D conventions. Thus, the joint angle convention's effect on the accuracy and reliability of RULA score measurement with IMUs is still unknown.

Therefore, in contrast to previous studies which used IMUs with 3D convention, this study's objective was to investigate the validity of an instrumented RULA assessment tool based on the kinematic models obtained by wearable IMUs and using both 2D and 3D joint angle conventions against the kinematic model obtained by the reference camera

motion-capture system. To this end, first, we quantified the accuracy of joint angles obtained by the IMU-system based on 3D and 2D conventions against the reference system through an experimental study with able-bodied individuals performing three manual material handling tasks. Then, we identified the convention resulting in higher reliability based on the repeatability of obtained RULA scores. Low-cost IMU-based instrumented RULA assessment tool could achieve high accuracy/repeatability, in contrast to simple observational methods proposed earlier, and can be widely adopted in industrial environments to reduce the risk of WMDs.

II. METHODS

A. EXPERIMENTAL PROCEDURES

Ten able-bodied individuals (all male, 25 ± 5 years old, 170 ± 5 cm, 69 ± 5 kg) with no history of back pain or musculoskeletal/neuromuscular injuries participated in the experiments. The Research Ethics Board Committee at the University of Alberta approved the study protocol (ID: Pro00083309), and written consent was obtained from all participants.

Each participant performed three manual material handling tasks, including six repetitions of task 1 (Figure 1(a)) and three repetitions of tasks 2 and 3 (Figures 1(b) and (c), respectively). The dimensions of the desks in Figure 1 were according to the NIOSH lifting equation manual [32]. For task 1 (packing), the participant performed trunk twisting to pick up an object from the initial position (desk 1) and dropping it over to the final destination (desk 2). Task 2 (package inspection) involved an asymmetric movement in which the participant bent in the sagittal plane to the knee height to pick up a box (desk 1) and place it on another desk at the head height (desk 2). In task 3 (reaching), the participant was asked to perform the following movements: standing motionless (N-pose) for five seconds and then reaching to an object at the head height (desk 1). In addition to the main tasks, participants were instructed to stand motionless for five seconds at the beginning and end of each repetition. The experimental study lasted about 15 seconds for each repetition, and we analyzed the full-range movement for each task, and not only the static standing postures at the beginning and the end of each repetition.

B. DATA COLLECTION

Reference Kinematic Model: To build the reference kinematic model, a motion-capture camera system (VICON, Oxford Metrics Group, UK) with eight cameras and a sampling frequency of 100 Hz was used to record the 3D trajectory of 15 retro-reflective markers attached to the anatomical landmarks of the body. The tracked anatomical landmarks were as follows: right and left Auricularis (head segment); seventh cervical vertebra or C7 (for head and trunk segments); Incisura Jugularis (for head and trunk segments); Processus Xiphoideus (for trunk segment); right and left Acromion

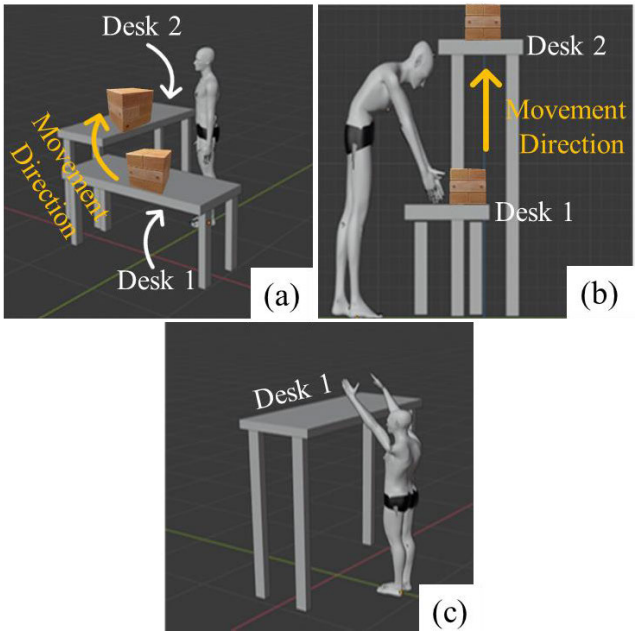

FIGURE 1. Three scenarios of manual material handling tasks. (a) task 1: Packing; (b) task 2: Package inspection; (c) task 3: Reaching an object.

(shoulder segment); right and left lateral/medial Humeral Epicondyle (upper-arm segment); right and left radial/ulnar Styloid (lower-arm segment). These markers were used as described in Sections II.D.1 and II.D.2 to calculated 3D and 2D joint angles.

IMU-based Kinematic Model: 17 IMUs (MTws, Xsens Technologies, the Netherlands) were used to record the participants' motion with a sampling frequency of 60 Hz. Each IMU included a tri-axial accelerometer (range: ±16 g), a tri-axial gyroscope (range: ±2000 °/s), and a tri-axial magnetometer (range: ±1.9 Gauss) and was attached to body segments using anti-allergic double-sided medical tape. After data collection, the IMU data were up-sampled to attain the sampling frequency of 100 Hz, similar to the camera system.

Data Collection: When the study coordinator pressed the "start/end" button in the custom-made software for data collection, an analogue trigger signal was generated by an Arduino and sent to both IMU and camera systems to start/end data collection. As such, both systems started/ended data collection at the beginning/end of each trial (i.e., each repetition of each task) separately but synchronously.

C. RULA SCORE IMPLEMENTATION

To calculate the RULA score, commonly, an observer identifies the posture score A (composed of upper-arm, lower-arm, wrist-twist, and wrist sub-scores) and the posture score B (composed of neck and trunk sub-scores). Each sub-score is obtained by comparing the segment's angular position with pre-defined angular thresholds in the RULA score sheet [11]. For instance, for trunk flexion/extension, angular positions of 0°-10° (0° means standing upright), 10°-20°, 20°-60°, >60° result in RULA sub-score of +1, +2, +3,

and +4, respectively. After calculating all sub-scores, they are combined and converted to the RULA score.

To evaluate the effect of joint angle convention on the measurement accuracy of instrumented RULA score during the material handling tasks, first, we calculated 3D or 2D joint angles (see Sections II.D.1 and II.D.2) using both IMU and camera systems. Then, we computed the RULA score at each time instant during the trials, according to Table 1 and RULA sheet [11]. Notably, for upper-arm, elbow, neck, and trunk flexion/extension, we compared the calculated angular positions for each segment with the pre-defined thresholds in the RULA sheet. The RULA score sheet did not define any numerical threshold for upper-arm adduction/abduction, shoulder adduction/abduction, lower-arm axial rotation, neck lateral bending, trunk adduction/abduction, and trunk axial rotation. For these joint angles, we considered the sub-score equal to 0 for angles equal to or smaller than 20° and equal to 1 for angles higher than 20°, similar to [33].

TABLE 1. Segments for which the RULA score was calculated along with the joint angles used for RULA score calculation. We used 20° as the threshold [33] for the undefined thresholds in the RULA sheet, meaning that for angular positions higher than 20°, a sub-score of +1 was given to the segment; otherwise, a sub-score of 0 was given to the segment.

Segment	Joint angles	Threshold
Upper-arm	Upper-arm flexion/extension	From RULA sheet [11]
	Upper-arm adduction/abduction	> 20° : +1
	Shoulder adduction/abduction	> 20° : +1
Lower-arm	Elbow flexion/extension	From RULA sheet
	Lower-arm axial rotation	> 20° : +1
Neck	Neck flexion/extension	From RULA sheet
	Neck lateral bending	> 20° : +1
Trunk	Trunk flexion/extension	From RULA sheet
	Trunk adduction/abduction	> 20° : +1
	Trunk axial rotation	> 20° : +1

D. JOINT ANGLE CALCULATION

Table 1 identifies the joint angles required for RULA score calculation and not the kinematic model that was used for data collection (described in Section II.D.1 and II.D.2 for 3D and 2D conventions, respectively). To measure 3D and 2D joint angles, the position of the markers attached to anatomical landmarks has been tracked with both IMU-based and camera-based systems. Then, the JCS convention (according to the ISB recommendations) and a planar projection method have been used to calculate 3D and 2D joint angles, respectively. Finally, the targeted joint angles (Table 1) were used to calculate the RULA score based on the 2D and 3D conventions.

1) 3D JOINT ANGLES

3D joint angles were obtained based on the JCS convention [28] and using anatomical coordinate systems defined in ISB recommendations [29], [30]. To this end, a segmental kinematic model was created using both IMU and camera data. For the camera-based segmental kinematic model, a 3D model was constructed based on the anatomical landmarks suggested by the ISB for upper [29], [30], as detailed in Table 1, except for the head, shoulder, and trunk segments. The reason is that the ISB recommendations did not define the head and shoulder segments, and also, the T8 marker, required for trunk segment construction, was missed by the camera system due to occlusion in most trials. Thus, we used the midpoint between C7 and Incisura Jugularis and right and left Auricularis anatomical landmarks to construct the head segment. We used the angles obtained from the 2D convention in the RULA score calculation for the shoulder segment. Moreover, C7, Incisura Jugularis, and Processus Xiphoideus were used to construct the local anatomical coordinate system of the trunk segment.

For the IMU-based segmental kinematic model, a 3D model was obtained by the Xsens-MVN Analyze software (Xsens Technologies, The Netherlands). Using Xsens proprietary sensor fusion algorithm for orientation estimation, the MVN Analyze software provided kinematic parameters of a 23-segment body model, including segments' orientation, joints' center position, and the 3D joint angles of the 22 joints as detailed in [34].

2) 2D JOINT ANGLES

A planar projection method similar to [31] was used for 2D joint angle calculation. To this end, first, joint centers were determined based on the anatomical markers (Figure 2(a)) as follows: head (point 1): midpoint of right and left Auricularis; neck (point 2): C7; right/left shoulder (points 4 and 5): right/left Acromion; right/left elbow (points 6 and 7): midpoint of right/left Lateral Humeral Epicondyle and right/left Medial Humeral Epicondyle; right/left wrist (points 8 and 9): midpoint of right/left Radial Styloid and right/left Ulnar Styloid. The sagittal, frontal, and transverse planes of the body were then defined, as shown in Figure 2(b), to locate the segments' angular position required for the RULA assessment tool. The sagittal plane was defined to be perpendicular to the *shoulder vector*. The *shoulder vector* was defined as a line connecting the right shoulder to the left shoulder (point 5 to 4). The frontal plane was parallel to the *shoulder vector* and passed through the *trunk vector*. The *trunk vector* was defined as a line connecting the spine base (point 3) to C7 (point 2). The transverse plane was considered to be the ground.

The neck flexion/extension angle was calculated as the angle between the projection of the *neck vector*, defined as a line connecting the head (point 1) to C7 (point 2), and the *trunk vector* in the sagittal plane. The neck lateral bending was computed as the angle between the *neck and shoulder vectors* in the frontal plane. The trunk flexion/extension was calculated as the angle between the *trunk vector* and the vertical direction in the sagittal plane. The trunk lateral bending angle was measured as the angle between the projections of the *shoulder vector* and *hip vector*, defined as a line passing through the right and left hips joint centers (points 10 and 11)

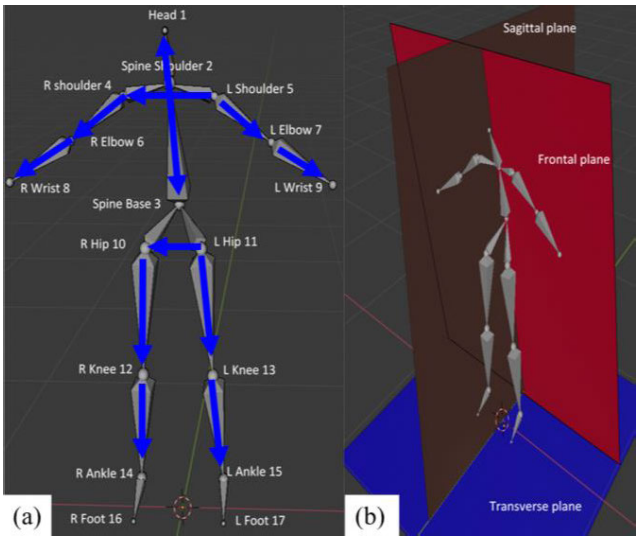

FIGURE 2. Illustration of the (a) joints center positions (the number after each joint's name indicates the point number referred to in the text) and (b) body anatomical planes used in the 2D joint angle calculation convention.

in the frontal plane. The trunk rotation was defined as the angle between the projections of the *shoulder vector* and the *hip vector* in the transverse plane.

The upper-arm flexion/extension was calculated as the angle between the projections of the *trunk vector* and the *upper-arm vector* in the sagittal plane. The *upper-arm vector* was defined as a vector directed from the shoulder (points 4 and 5) to the elbow (points 6 and 7). The upper-arm adduction/abduction was computed as the angle between the projection of the *upper-arm vector* in the frontal plane and the *trunk vector*. The elbow flexion/extension angle was calculated as the angle between the *upper-arm vector* and *lower-arm vector*, defined as a line that passes through the elbow (points 6 and 7) to the wrist (points 8 and 9) in the sagittal plane. The upper-arm rotation was also calculated as the angle between the *shoulder vector* and the *lower-arm vector* projected into the transverse plane. Finally, the shoulder addiction/abduction angle was computed as the angle between the *shoulder vector* and the *trunk vector* in the frontal plane. Note that according to the RULA sheet [11], the upper-arm (Figure 2: vector connecting point 4/5 to 6/7) and shoulder (Figure 2: vector connecting point 5 to 4) are different segments. Therefore, the upper-arm abduction and raising the shoulder (abduction/adduction) contribute to the RULA score separately. Thus, as shown in Table 1, we considered separate sub-scores for upper-arm and shoulder adduction/abduction in line with the RULA score sheet.

E. DATA ANALYSIS

The data analysis was done in MATLAB (MathWorks, USA). All IMU and camera data were filtered using a 3rd-order one-dimensional median filter before any data processing. Each repetition of each task was analyzed separately. Offset, RMSE before removing offset (RMSE^{+}), and RMSE after removing offset (RMSE^{-}) of joint angles were calculated, based on the error between the IMU-based and camera-based angles, to quantify the accuracy of the IMU-based system for measuring 3D and 2D joint angles. Also, the agreement between IMU-based and camera-based RULA scores obtained by 2D and 3D kinematic models was quantified by calculating the proportion agreement index and Cohen's Kappa coefficient on a sample-to-sample basis [35]. The z-test was used to identify if the agreement between the two systems was accidental.

To assess the intra-participant repeatability, the intra-class correlation coefficient (ICC) [36] was calculated for the three trials of each participant during each task. For the ICC, the degree of absolute agreement for three independent measurements under the fixed levels of the column factor (two-way mixed model, interaction absent) was calculated. The closer the value of ICC to 1, the more repeatable the method. Moreover, the inter-participant variability of the joint angle RMSEs was tested using a multiple-sample test for equal variances (Bartlett test) at the significance level of 5%. The Bartlett test showed that the variances of RMSEs were significantly ($p<0.05$) different for all tasks. Thus, nonparametric Friedman's test, along with post-hoc multiple comparisons (using Bonferroni correction), were employed to detect significant differences among the RMSEs of joint angles in each task at the significance level of 5%.

III. RESULTS

We have collected data from 12 participants during our experimental study. Nevertheless, due to the loss of spatial data (occlusion of motion-capture cameras) or temporal synchronization, we were only able to use the data of 10 participants. In the current section, we report the major findings of the experimental study, while Section IV: Discussion, details the implications of the findings, places the obtained results in the literature context, and addresses the limitations and future directions for the current study.

A. 3D JOINT ANGLES

A representative plot of joint angles obtained based on 3D convention during task 1 shows that the measured joint angles with the IMU-based system and their reference counterpart had similar patterns (Figure 3(a)). However, there was always an offset between the two systems, and the value of the offset error was different among different segments, as presented in Table 2. Also, a representative plot of RULA scores for one trial during the three tasks showed that the RULA scores obtained based on 3D convention using IMU-based and camera-based systems had similarities and differences (Figure 4(a)). Note that the presented angles/RULA score in Figures 3 and 4 may not be an actual representative for all participants and demonstrate the pattern of joint angles/RULA score in general.

Figure 5 shows the joint angles RMSE^{+}s between the IMU-based and camera-based kinematic models for the

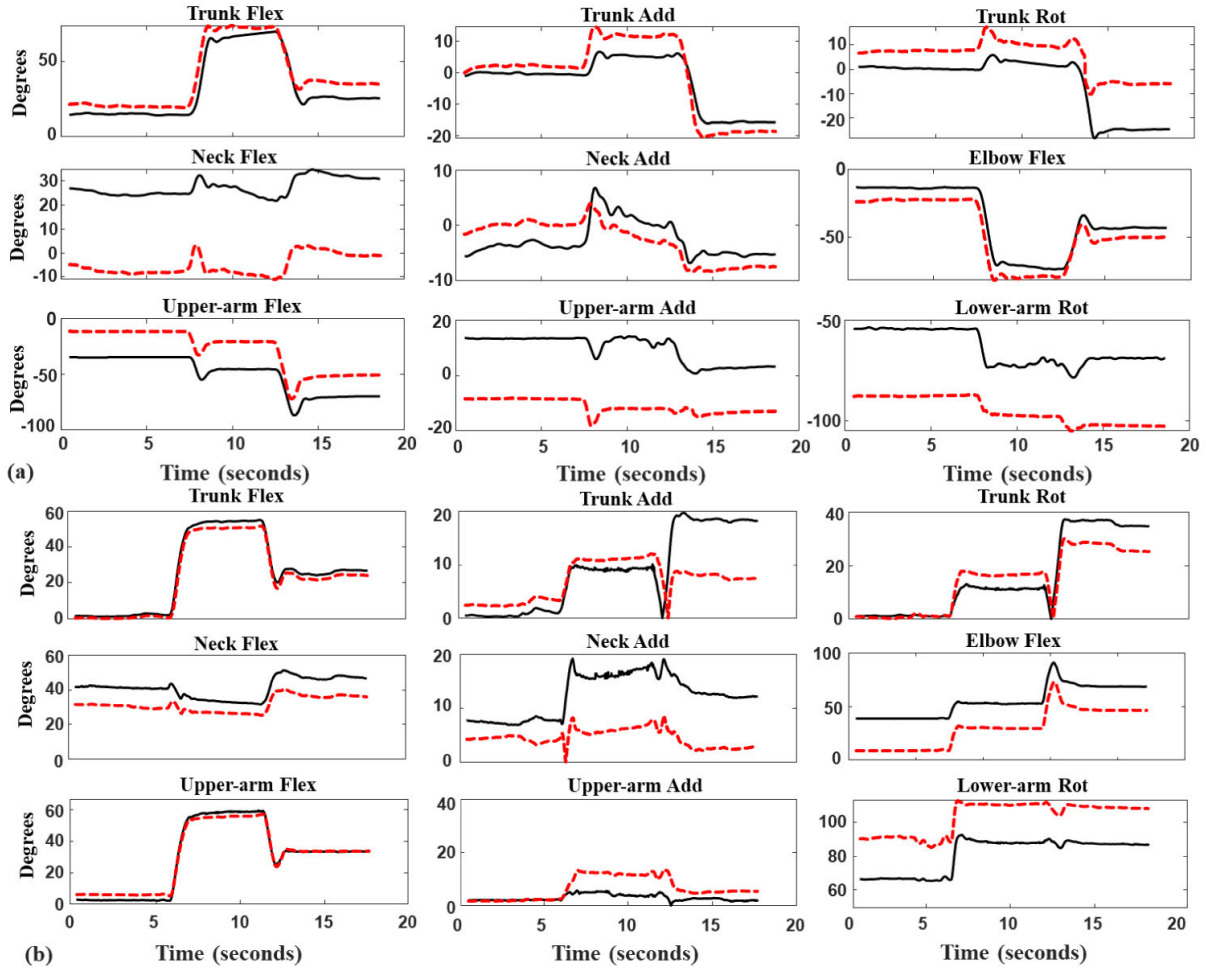

FIGURE 3. A representative plot of the joint angles of the trunk, neck, and right upper-arm, right lower-arm, and right elbow obtained using the (a) 3D convention and (b) 2D convention (task 1, trial 1, participant 1). Shoulder adduction/abduction was not presented to provide comparable graphs between both conventions. Solid black and dashed red lines show the angles obtained by camera-based and IMU-based systems, respectively. Terms Flex, Add, and Rot indicate flexion/extension, adduction/abduction, and axial rotation, respectively. The presented angles may not be an actual representative for all participants and are depicted to demonstrate the pattern of joint angles in general.

3D convention during tasks 1, 2, and 3. For all tasks, the median RMSE$^+$s were lower than or close to 10° for trunk and neck joint angles, except for neck flexion/extension. Also, according to Table 2, for the trunk, neck, and elbow flexion/extension as well as upper-arm adduction/abduction and rotation angles, the median offset errors were 1.8 to 5.3 times greater than the median RMSE$^-$s in task 1. In tasks 2 and 3, trunk, neck, and elbow flexion/extension, as well as upper-arm adduction/abduction and rotation angles, had a larger median offset error than that of RMSE$^-$. Notably, for all three tasks, elbow flexion/extension and upper-arm rotation angles had offset errors of higher than 20°, while the RMSE$^-$s were smaller than 11°. Moreover, for all joints, except for the elbow flexion/extension and upper-arm rotation angles, the interquartile ranges of RMSE$^-$s were lower than 6.3° among all tasks, while the interquartile ranges of the offset errors were lower than 11.4°. Furthermore, the elbow flexion/extension and upper-arm rotation angles had the lowest inter-participant reliability (largest interquartile range), as shown in Figure 5.

Table 3 shows that according to the Landis and Koch scale [35], the RULA scores measured by IMU-based and camera-based systems using the 3D convention had a ''moderate'' agreement during all tasks. The z-test showed that the high agreement between the two systems during all tasks and for both body sides was not accidental at a significance level of 5%.

B. 2D JOINT ANGLES

A representative plot of joint angles obtained based on 2D convention during task 1 shows that the measured joint angles with the IMU-based system and their reference counterpart had similar patterns (Figure 3(b)). However, for neck and elbow flexion/extension, neck adduction/abduction, and upper-arm rotation angles, there was an offset between the two systems. Also, a representative plot of RULA scores

TABLE 2. Offset and RMSE^{-} (after removing the offset) of the joint angles obtained by the 3D convention using the IMU-based system against the camera-based system presented as median (interquartile range) among all participants. Terms Flex, Add, and Rot indicate flexion/extension, adduction/abduction, and axial rotation, respectively.

Joint angles	Body side	Offset			RMSE−		
		Task 1	Task 2	Task 3	Task 1	Task 2	Task 3
Trunk Flex		8.0(7.6)	8.7(7.1)	8.6(9.9)	4.1(1.5)	5.4(1.6)	2.0(1.1)
Trunk Add		2.9(3.7)	3.2(1.9)	2.6(2.5)	4.6(2.7)	2.5(1.5)	1.7(1.1)
Trunk Rot		5.4(5.3)	4.6(6.0)	4.2(4.9)	4.8(2.4)	3.4(1.9)	1.5(1.9)
Neck Flex		14.0(5.8)	12.2(8.2)	11.7(9.7)	3.7(3.3)	7.3(4.3)	7.2(4.6)
Neck Add		3.6(6.7)	2.5(3.9)	2.3(3.9)	4.2(4.1)	2.0(1.8)	2.3(1.4)
Elbow Flex	Right	23.7(18.4)	23.7(19.6)	25.9(17.4)	4.5(4.7)	7.0(3.0)	8.3(5.4)
	Left	22.6(12.8)	22.5(9.4)	23.8(12.8)	6.4(6.5)	7.9(3.6)	9.9(2.9)
Upper-arm Flex	Right	7.1(7.7)	6.6(10.1)	7.3(8.2)	5.2(2.9)	8.0(5.1)	8.5(6.3)
	Left	7.2(7.7)	9.6(11.4)	8.1(6.7)	5.1(3.7)	7.4(5.4)	8.2(6.0)
Upper-arm Add	Right	2.5(3.2)	2.8(3.2)	2.9(3.7)	4.2(3.7)	4.1(2.2)	4.9(3.2)
	Left	6.1(3.5)	5.3(2.7)	5.9(2.5)	3.47(2.2)	6.1(6.2)	5.0(3.2)
Upper-arm Rot	Right	23.0(17.3)	22.2(14.4)	24.1(24.4)	10.80(9.5)	6.8(6.8)	7.6(18.9)
	Left	28.6(19.0)	25.2(12.5)	27.5(14.4)	9.47(7.1)	7.9(5.9)	5.0(9.3)

TABLE 3. Proportion agreement index (Po), linear weighted Cohen's kappa, and p-value of z-test, and degree of agreement based on Landis and Koch scale [35], between the RULA scores obtained by IMU-based and camera-based kinematic models using the 3D convention. The results are presented as 50th (25th, 75th) percentile among participants.

Task	Body side	Po	Cohen's kappa	Agreement	p-value	Null hypothesis
1	Right	0.73(0.68,0.81)	0.45(0.29,0.55)	Moderate	< 0.05	Rejected
	Left	0.73(0.66,0.81)	0.43(0.26,0.52)	Moderate	< 0.05	Rejected
2	Right	0.73(0.66,0.81)	0.51(0.48,0.61)	Moderate	< 0.05	Rejected
	Left	0.79(0.76,0.85)	0.48(0.40,0.68)	Moderate	< 0.05	Rejected
3	Right	0.86(0.72,0.90)	0.60(0.36,0.75)	Moderate	< 0.05	Rejected
	Left	0.83(0.75,0.88)	0.55(0.37,0.67)	Moderate	< 0.05	Rejected

The Cohen's kappa less than 0 indicates a "poor" agreement, 0 and 0.20 indicates a "slight" agreement, 0.21 and 0.40 a "fair" agreement, 0.41 and 0.60 a "moderate" agreement, 0.61 and 0.80 a "substantial" agreement, and values of 0.81 and higher indicate a "perfect" agreement [35].

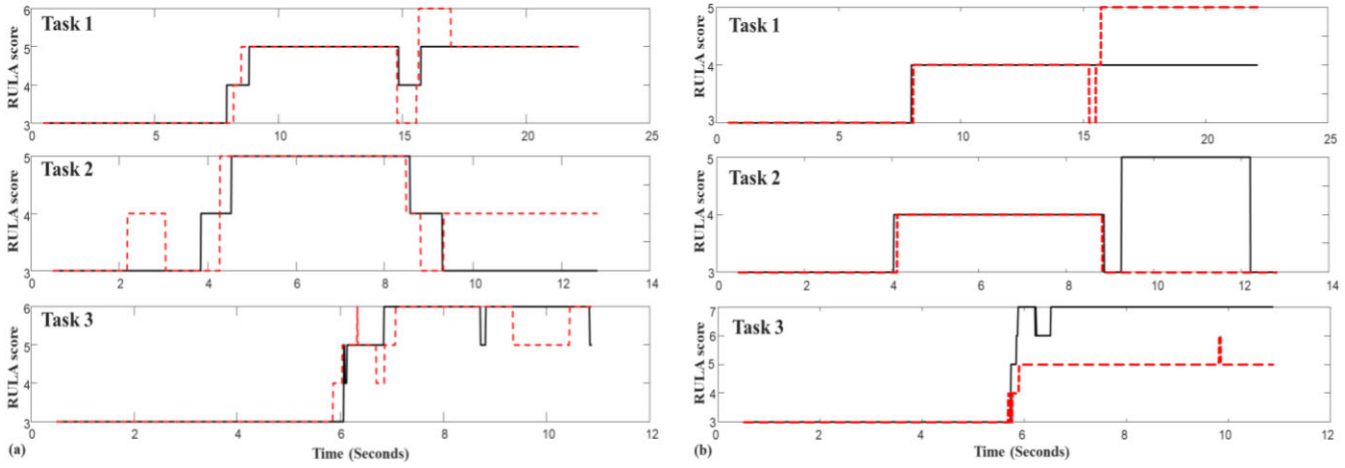

FIGURE 4. A representative plot of the RULA scores was obtained using the 3D convention for one complete trial, including five seconds of quiet standing, performing the task, and then five seconds of quiet standing (tasks 1, 2, 3, trial 1, participant 1). Solid black and dashed red lines show the RULA score obtained by camera-based and IMU-based systems, respectively. Terms Flex, Add, and Rot indicate flexion/extension, adduction/abduction, and axial rotation, respectively. The presented angles may not be an actual representative for all participants and are depicted to demonstrate the pattern of joint angles in general.

for one trial during the three tasks showed that the RULA scores obtained based on 2D convention using IMU-based and camera-based systems had similarities and differences (Figure 4(b)).

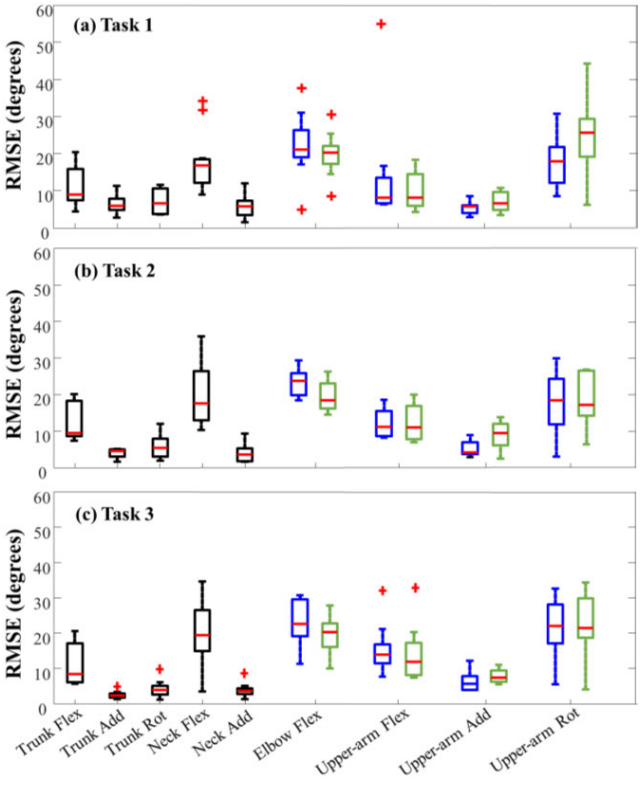

FIGURE 5. Root-mean-square error (RMSE$^+$: without removing the offset) of the 3D convention between the IMU-based and camera-based systems shown as boxplots over the results of 10 participants for (a) task 1, (b) task 2, and (c) task 3. The boxplots for the trunk and neck are shown in black, those for the right side are shown in blue, and those for the left side are shown in green. Terms Flex, Add, and Rot indicate flexion/extension, adduction/abduction, and axial rotation, respectively.

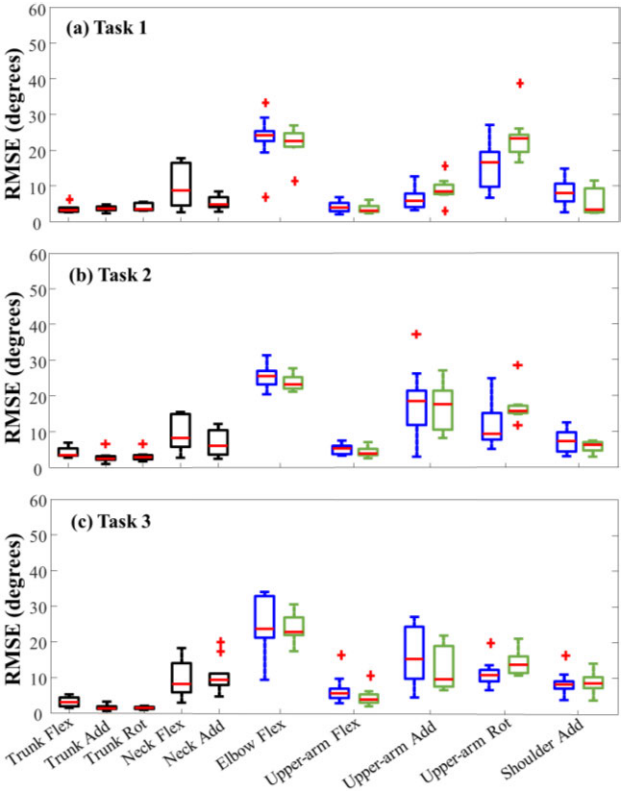

FIGURE 6. Root-mean-square error (RMSE$^+$: without removing the offset) of the 2D convention between the IMU-based and camera-based systems shown as boxplots over the results of 10 participants for (a) task 1, (b) task 2, and (c) task 3. The boxplots for the trunk and neck are shown in black, those for the right side are shown in blue, and those for the left side are shown in green. The terms Flex, Add, and Rot indicate flexion/extension, adduction/abduction, and axial rotation, respectively.

Figure 6 shows the joint angles RMSE$^+$s between the IMU-based and reference camera-based kinematic models for joint angles obtained by the 2D convention during the three tasks. The median RMSE$^+$s were lower than or close to 10° for trunk and neck joint angles for all tasks. Also, according to Table 4, for neck and elbow flexion/extension, upper-arm adduction/abduction, and shoulder rotation angles, the median offset errors were 2.7 to 9.6 times greater than the median RMSE$^-$s in task 1. However, in contrast to the 3D convention, the trunk angles obtained by the 2D convention had offset errors nearly 2 times smaller than the RMSE$^-$s. For tasks 2 and 3, neck and elbow flexion/extension, upper-arm adduction/abduction, and shoulder rotation angles had a larger median offset error than that of RMSE$^-$. Notably, for all three tasks, neck and elbow flexion/extension and upper-arm rotation angles had offset errors of higher than 10°, while the RMSE$^-$s were smaller than 17°. Moreover, according to Table 4, the upper-arm adduction/abduction and rotation angles had the lowest inter-participant reliability, i.e., the highest offset and RMSE$^-$ interquartile ranges, respectively, among three tasks (15.2° and 17.7°). At the same time, the trunk angles, as well as the upper-arm flexion/extension, had the highest inter-participant reliability, i.e., offset and RMSE$^-$ interquartile ranges were lower than 4.2°.

Furthermore, Table 5 shows that according to the Landis and Koch scale [35], the RULA scores measured by IMU-based and camera-based systems using the 2D convention had a ''substantial'' agreement during tasks 1 and 3 and a ''moderate'' agreement during task 2. The z-test showed that the high agreement between the two systems during all tasks and for both body sides was not accidental at a significance level of 5%.

C. COMPARISON OF 3D AND 2D CONVENTIONS

Table 6 shows a comparison between the 3D and 2D conventions by comparing the RMSE$^+$ associated with each joint angle (measured against the camera-based system). In general, the 2D joint angle convention had significantly ($p<0.05$) smaller RMSE$^+$s compared to the 3D convention in tasks 1, 2, and 3 for 6, 7, and 9 joint angles (out of 13 joint angles), respectively. In particular, for trunk angles, Figures 5 and 6, as well as Table 6, show that the 2D convention was preferred, as the RMSE$^+$s associated with trunk flexion/extension, adduction/abduction, and rotation angles of the 2D convention were significantly ($p<0.05$) smaller than those of the 3D convention for all tasks. Notably, the median RMSE$^+$ in measuring the trunk angles using 2D convention never

TABLE 4. Offset and RMSE$^-$ (after removing the offset) of the joint angles obtained by the 2D convention using the IMU-based system against the camera-based system presented as median (interquartile range) among all participants. Terms Flex, Add, and Rot indicate flexion/extension, adduction/abduction, and axial rotation, respectively.

Joint angles	Body side	Offset			RMSE–		
		Task 1	Task 2	Task 3	Task 1	Task 2	Task 3
Trunk Flex		1.7(0.2)	2.5(4.4)	2.1(2.4)	3.1(2.1)	3.3(1.7)	3.1(2.4)
Trunk Add		1.5(1.9)	2.6(3.0)	1.4(1.9)	3.4(1.6)	2.3(0.7)	1.4(1.6)
Trunk Rot		1.9(2.2)	0.9(1.5)	0.9(1.4)	4.8(1.8)	2.6(2.4)	1.5(1.1)
Neck Flex		10.7(10.8)	11.5(10.6)	10.1(9.4)	2.1(1.3)	2.7(1.5)	2.2(2.4)
Neck Add		3.3(3.6)	2.2(3.6)	2.9(3.5)	4.5(2.1)	3.5(5.2)	8.3(4.7)
Elbow Flex	Right	28.8(8.6)	29.5(8.7)	29.9(8.4)	3.1(3.5)	3.7(3.7)	5.8(9.2)
	Left	24.9(5.7)	26.4(6.4)	27.0(5.1)	2.6(3.3)	3.1(5.5)	6.2(6.4)
Upper-arm Flex	Right	3.1(2.9)	3.3(2.6)	3.0(3.9)	3.9(2.6)	5.2(3.6)	5.8(4.0)
	Left	1.9(2.4)	2.4(2.8)	2.4(2.6)	3.0(2.0)	4.0(2.6)	3.7(3.8)
Upper-arm Add	Right	5.9(7.5)	4.1(8.8)	6.5(9.1)	4.6(3.2)	11.0(11.9)	15.0(17.7)
	Left	7.5(5.1)	8.0(5.1)	9.0(5.2)	4.3(4.5)	13.1(5.1)	13.8(16.9)
Upper-arm Rot	Right	11.4(10.4)	9.2(8.7)	9.4(8.6)	4.3(4.9)	7.4(4.7)	12.5(5.1)
	Left	19.9(11.7)	18.4(15.2)	12.5(7.2)	5.7(6.2)	9.7(8.1)	16.6(6.7)
Shoulder Add	Right	6.3(7.4)	6.6(8.8)	6.1(9.2)	4.8(3.6)	7.2(2.5)	3.8(7.9)
	Left	1.9(6.6)	2.8(6.3)	1.9(3.2)	2.6(1.4)	6.3(3.3)	8.3(6.7)

TABLE 5. Proportion agreement index (Po), linear weighted Cohen's kappa, and p-value of z-test, and degree of agreement based on Landis and Koch scale [35], between the RULA scores obtained by IMU-based and camera-based kinematic models using the 2D convention. The results are presented as 50th (25th, 75th) percentile among participants.

Task	Body side	Po	Cohen's kappa	Agreement	p-value	Null hypothesis
1	Right	0.90(0.85,0.92)	0.72(0.58,0.77)	Substantial	< 0.05	Rejected
	Left	0.90(0.87,0.93)	0.74(0.56,0.80)	Substantial	< 0.05	Rejected
2	Right	0.85(0.79,0.90)	0.54(0.40,0.74)	Moderate	< 0.05	Rejected
	Left	0.86(0.80,0.90)	0.59(0.49,0.76)	Moderate	< 0.05	Rejected
3	Right	0.90(0.80,0.90)	0.80(0.60,0.82)	Substantial	< 0.05	Rejected
	Left	0.90(0.80,0.94)	0.80(0.58,0.86)	Substantial	< 0.05	Rejected

The Cohen's kappa less than 0 indicates a "poor" agreement, 0 and 0.20 indicates a "slight" agreement, 0.21 and 0.40 a "fair" agreement, 0.41 and 0.60 a "moderate" agreement, 0.61 and 0.80 a "substantial" agreement, and values of 0.81 and higher indicate a "perfect" agreement [35].

exceeded 5°, while for trunk flexion/extension obtained by 3D convention, median RMSE$^+$ of nearly 10° were observed. Also, the interquartile ranges associated with 2D trunk angles tended to be smaller than the 3D angles. Similarly, for the neck flexion/extension angle, the median RMSE$^+$ of the 3D convention was nearly 2 times greater than those of the 2D convention for all tasks. On the other hand, for neck adduction/abduction angle, similar RMSE$^+$s were obtained by both conventions, except for task 3, where the RMSE$^+$s obtained by the 3D convention were significantly smaller.

In contrast to trunk and neck angles, the elbow flexion/extension angle, obtained using 3D convention, resulted in significantly ($p<0.05$) lower RMSE$^+$s compared to the 2D convention for tasks 1 and 2. For the same angle and task 3, RMSE$^+$s of the right-side angles associated with the 2D convention were significantly ($p<0.05$) smaller compared to the 3D convention, and no significant difference was observed between the left-side RMSE$^+$s. Also, the upper-arm flexion/extension angle obtained by the 2D convention resulted in significantly smaller RMSE$^+$ compared to the 3D convention for both sides and all tasks. Notably, Figures 5 and 6 show that for the 2D convention, the RMSE$^+$s were less than 5° among all tasks (for both sides), while for 3D conventions, RMSE$^+$s were close to 10° or higher.

On the other hand, the upper-arm adduction/abduction angle, obtained by 3D convention, resulted in significantly smaller RMSE$^+$ compared to the 2D convention, except for the right-side in task 1. Notably, for tasks 2 and 3 with a smaller range of motions in the frontal plane, the 3D convention showed to be more reliable by achieving smaller interquartile ranges of error compared to 2D. For upper-arm rotation during task 1, no significant difference was observed between the two conventions, while for task 3, the 2D convention resulted in a significantly ($p<0.05$) lower error than the 3D convention.

Tables 3 and 5 show that the obtained RULA scores with the two conventions had Cohen's kappa coefficients ranged from 0.43 to 0.60 for 3D and 0.54 to 0.80 for 2D. In other words, a ''substantial'' agreement between IMU-based and camera-based systems was achieved for two tasks using the

TABLE 6. Comparison between the accuracy of the 2D and 3D conventions for the three manual material handling tasks. The accuracy of the two conventions was defined as their RMSEs measured against the camera-based system before removing the offset (RMSE+) and compared using statistical analysis (p-values of the comparisons are reported). †indicates significantly lower RMSE+s for the 2D convention, while ‡indicates significantly lower RMSE+s for the 3D convention. The terms Flex, Add, and Rot indicate flexion/extension, adduction/abduction, and axial rotation, respectively.

Joint angles	Body side	Task 1	Task 2	Task 3
Trunk Flex		<0.001†	<0.001†	<0.001†
Trunk Add		<0.001†	0.011†	<0.001†
Trunk Rot		<0.001†	0.035†	<0.001†
Neck Flex		<0.001†	<0.001†	<0.001†
Neck Add		0.723	0.050	<0.001‡
Elbow Flex	Right	<0.001‡	0.001‡	<0.001†
	Left	<0.001‡	<0.001‡	0.334
Upper-arm Flex	Right	<0.001†	<0.001†	<0.001†
	Left	<0.001†	<0.001†	<0.001†
Upper-arm Add	Right	0.076	<0.001‡	<0.001‡
	Left	0.020‡	<0.001‡	<0.001‡
Lower-arm Rot	Right	0.244	0.001†	<0.001†
	Left	0.362	0.513	<0.001†

2D convention only. Moreover, Table 7, which provides the ICC values among repeated trials of each participant, shows that the 2D convention was more repeatable than the 3D in all tasks except for the left-side in task 3.

IV. DISCUSSION

Wearable IMUs proved to be a powerful tool for ambulatory measurement of human motion, focusing on lower-limb or upper-limb. For instance, Qiu *et al.* [37] proposed a distributed IMU system to analyze lower-limb motion and measure the swing/stance phase, step size, and segment positions. More recently, Anwary *et al.* [38] performed an extensive experimental study to determine the optimal location for the foot-mounted IMU toward building an automatic system for accurate and repeatable gait analysis. Also, Sun *et al.* [39] proposed the application of wearable IMUs to conduct gait-based identity recognition for the elderly population. However, these works, or their counterparts for upper-limb such as [40], [41], were focused on algorithm development with wearable IMUs toward measuring clinically meaningful parameters, especially for among elderly population or patients, and have not involved the development of an instrumented ergonomic risk assessment tool for the healthy population in industrial environments.

Wearable IMUs have a great potential for in-field measurement of RULA scores to improve the ergonomic risk assessment's accuracy and reliability. Yet, few studies [25], [26], [42] have proposed the application of IMUs for RULA score calculation toward ergonomic risk assessment based on various biomechanical models with different degrees of freedom. Also, the body segment angles defined in the RULA score are not the same as the 3D Cardan angles measured by IMUs in biomechanics research. Thus, it is unknown which

TABLE 7. The intraclass correlation coefficient (ICC) and lower and upper bound of 95% confidence interval of the median RULA score among repeated trials of each participant.

Task	Body side	3D Convention	2D Convention
1	Right	0.82(0.55,0.95)	0.87(0.70,0.96)
	Left	0.89(0.75,0.97)	0.93(0.84,0.98)
2	Right	0.91(0.72,0.98)	0.92(0.87,0.99)
	Left	0.82(0.48,0.95)	0.95(0.77,0.98)
3	Right	0.90(0.69,0.98)	0.95(0.65,0.96)
	Left	0.94(0.83,0.99)	0.87(0.85,0.98)

ICC shows poor (ICC < 0.5), moderate (0.50 < ICC < 0.75), good (0.75 < ICC < 0.90), and excellent (0.90 < ICC < 1) repeatability as defined in [36].

joint angle convention obtains better accuracy and reliability for the IMU-based RULA scores. This study experimentally investigated the accuracy of a wearable IMU-based instrumented RULA assessment tool against the kinematic model obtained by a camera motion-capture system, using both 3D (using JCS according to ISB recommendations) and 2D (using planar projection of angles) joint angle calculation conventions during three manual material handling tasks.

A. ACCURACY OF JOINT ANGLE CONVENTIONS

We compared the 3D and 2D conventions for the joint angles associated with the trunk segment and observed larger errors for the 3D convention (Figures 5 and 6). In particular, the trunk flexion/extension angle was measured as the angle between *trunk vector* and vertical direction for the 2D convention, which only relied on the position of two anatomical landmarks, i.e., head (point 1 in Figure 2) and C7 (point 2 in Figure 2). On the other hand, for the 3D convention, trunk and pelvis anatomical local frames must be calculated, which requires the position of seven anatomical landmarks. Thus, small differences between the position of anatomical landmarks obtained by the Xsens-MVN Analyze software and camera system caused by marker displacements due to skin movement artifact would have a greater impact on the joint angles calculated via the 3D convention. A similar pattern was observed for the neck flexion/extension angle. Another reason for having the largest error in trunk and neck flexion/extension angles during tasks 2 and 3 was that during these two tasks, the range of motion in the sagittal plane was larger compared to the other planes, i.e., the primary motion of the trunk and neck was in the sagittal plane. In contrast to trunk and neck angles, none of the conventions always resulted in smaller errors for elbow and upper-arm angles (Table 6).

To better characterize the errors obtained by the two conventions, we calculated offset and RMSE^{-} (after removing the offset error) (Tables 2 and 4). The fixed offset error was caused by the IMU calibration, while errors in orientation estimation with IMU or soft tissue artifact contributed to the RMSE^{-}. The offset error could be eliminated by instructing

the participants to hold a specific posture, e.g., N-pose, at the beginning of the data acquisition, and then removing the offset between two systems. Therefore, to identify a joint angle calculation convention, we focus on $RMSE^{-}$s. Comparing Tables 2 and 4 reveals that the 2D convention resulted in errors with lower $RMSE^{-}$s in all tasks, except for the neck and upper-arm adduction/abduction angles, and upper-arm rotation angle in tasks 2 and 3.

Robert-Lachaine *et al.* [43] evaluated the differences between the joint angles obtained by the Xsens software and the reference camera-based system using the 3D convention during simple functional tasks such as head, trunk, and upper-arm flexion/extension, adduction/abduction, and rotation. They showed that the soft-tissue artifact associated with both IMUs and markers during manual material handling tasks could negatively affect the calculated joint angles' accuracy and reliability. They also showed that the IMU calibration process and the anthropometric measurements required for obtaining anatomical local coordinate systems according to ISB recommendations [29], [30] could contribute to the observed errors, mostly in terms of a constant offset. However, the impact of the joint angle calculation convention on the accuracy and reliability of the results has not been assessed.

They reported a mean RMSE of 40.2° for the upper-arm adduction/abduction, which was larger than the median error $RMSE^{+}$ of the same angle obtained by the 3D convention in our study for the left side (9.5°). This large difference could be a result of (1) measuring the glenohumeral joint to represent the upper-arm joint center position and (2) having a longer experimental duration, which may increase the orientation estimation error in [43]. Also, the largest upper-arm adduction/abduction $RMSE^{+}$ obtained by 2D convention (18.5°) in our study was smaller than the one reported in [43] using the 3D convention. Conversely, the elbow flexion/extension median $RMSE^{+}$s obtained by 3D and 2D conventions (23.7° and 25.5°, respectively) in our study were larger than the mean RMSE (6.2°) reported in [43]. These large errors in our study were mainly due to the offset between the IMU-based and camera-based systems. Also, in contrast to [43], where only single-axis motions were evaluated, we assessed the IMU system during complex multi-dimensional tasks.

B. IN-FIELD RULA SCORE MEASUREMENT

As the effect of the joint angle calculation convention on the RULA score calculation has not been assessed, we reported the agreement between RULA scores obtained by the IMU-based and camera-based systems for 2D and 3D conventions. Using the 3D convention, for tasks 1 and 2, with more complex motions than task 3, a "moderate" agreement was obtained between RULA scores measured via IMU-based and camera-based systems. At the same time, using the 2D convention, for tasks 1 and 3, a "substantial" agreement was obtained between RULA scores measured via IMU-based and camera-based systems, while a "moderate" agreement was obtained for task 2 (Table 5). The differences between the agreements of right and left sides for all tasks in Tables 3 and 5 were likely due to the bilateral asymmetry at the destination workstations.

Also, we evaluated the repeatability of the two conventions by measuring the ICC among repeated trials of one participant. The ICCs ranged from 0.82 to 0.94 ("good" and "excellent" according to [36]) for 3D and 0.87 to 0.95 ("good" and "excellent," according to [36]) for 2D conventions (Table 7). In other words, the 2D convention tended to be more repeatable than the 3D in all tasks except for the left-side in task 3. Therefore, the 2D convention could be considered a more accurate and repeatable convention than the 3D convention for joint angle and RULA score measurement.

C. VALIDITY OF RULA SCORES COMPUTED BY IMU SYSTEM

According to Tables 2 and 4, for 3D and 2D conventions, the median of RMSEs among all participants and tasks ranged between 1.5° to 10.8° and 1.4° to 16.6°. At the same time, the pre-defined thresholds for calculating RULA sub-scores for upper-arm, lower-arm, neck, and trunk angles are 20°, 40°, 10°, and 20°, respectively. Thus, this level of error might not always affect the calculated RULA score. As a result, the agreement between IMU and camera systems were "moderate" or "substantial." Therefore, despite considerable RMSE of the IMU system in tracking the body segments' angular position, the accuracy of the RULA scores computed by IMUs was not poor in most cases.

Nevertheless, we used the Xsens-MVN Analyze as a commercial package to track the segments' angular position. Thus, the obtained RULA score by other IMU systems might have different accuracy. In general, to further improve the accuracy and reliability of the IMU system for in-field ergonomic risk assessment, we recommend the following:

1) A proper sensor fusion algorithm with high accuracy and reliability must be implemented to estimate the IMU orientation from its raw data. For instance, [44], [45] provided surveys on various sensor fusion algorithms.
2) An accurate and reliable sensor-to-segment calibration must be implemented to transform quantities such as joint angles from the IMU technical frame to the segment anatomical frame. See [46], [47] and [19], 20], [48] for examples of procedures developed for upper and lower extremities, respectively.
3) A proper calibration pose (N-pose or T-pose) must be included at the beginning of the data collection to remove the offset in the calculated joint angles.

D. LIMITATIONS AND FUTURE WORKS

A number of limiting factors must be mentioned. First, the IMU system's accuracy and reliability were evaluated for 10 male participants and three manual material handling tasks and should be further investigated. Notably, recruiting a larger sample size from both sexes and performing more complex

tasks in industrial environments is required before making any general conclusion about the accuracy and reliability of the IMU system in real-world scenarios. Second, the effect of muscle use and weight during manual material handling tasks were not considered in the current work as they could not be measured using IMUs. Third, the wrist joint angles were entered manually due to limited kinematic data.

Fourth, the RULA tool inherently lacks precision since the integer sub-scores are based on many thresholds, and the final score is much sensitive to the angle thresholds and accurate measurement around them. Besides, the RULA assessment tool does not consider all body joint angles and thus might not be an ideal tool for comprehensive ergonomic risk assessment. Therefore, in the future, the IMU system's accuracy and reliability must be evaluated for whole-body assessment tools, such as the Rapid Entire Body Assessment (REBA). Fifth, the IMUs inherently suffer from gyroscope drift and magnetic disturbance, which could have a drastic effect on the measured joint angles for long-duration tasks in industrial environments. Thus, the effect of IMU calibration on the accuracy and reliability of its estimated segment orientation must be investigated in the future, particularly for dynamic tasks and in the presence of ferromagnetic disturbances [49], [50].

ACKNOWLEDGMENT

The authors would like to thank the Neuromuscular Control and Biomechanics Laboratory members at the University of Alberta for their assistance during data collection, especially Aminreza Khandan, for his technical advice/assistance.

REFERENCES

[1] *Office Ergonomics*, Workers' Compensation Board Alberta, Edmonton, AB, Canada, 2007.
[2] L. Punnett and D. H. Wegman, "Work-related musculoskeletal disorders: The epidemiologic evidence and the debate," *J. Electromyogr. Kinesiol.*, vol. 14, no. 1, pp. 13–23, Feb. 2004.
[3] *IEA Triennial Report, 2000–2003*, Int. Ergonom. Assoc., Utrecht, The Netherlands, 2003.
[4] *Injuries at Work*, Canadian Community Health Survey (CCHS), Concord, MA, USA, 2003.
[5] P. Plantard, E. Auvinet, A.-S. Pierres, and F. Multon, "Pose estimation with a Kinect for ergonomic studies: Evaluation of the accuracy using a virtual mannequin," *Sensors*, vol. 15, no. 1, pp. 1785–1803, Jan. 2015.
[6] I. Balogh, P. Ørbaek, J. Winkel, C. Nordander, K. Ohlsson, and J. Ektor-Andersen, "Questionnaire-based mechanical exposure indices for large population studies–reliability, internal consistency and predictive validity," *Scandin. J. Work, Environ. Health*, vol. 27, no. 1, pp. 41–48, Feb. 2001.
[7] A. Choobineh, S. H. Tabatabaee, and M. Behzadi, "Musculoskeletal problems among workers of an iranian sugar-producing factory," *Int. J. Occupational Saf. Ergonom.*, vol. 15, no. 4, pp. 419–424, Jan. 2009.
[8] C. Trask, K. Teschke, J. Village, Y. Chow, P. Johnson, N. Luong, and M. Koehoorn, "Measuring low back injury risk factors in challenging work environments: An evaluation of cost and feasibility," *Amer. J. Ind. Med.*, vol. 50, no. 9, pp. 687–696, 2007.
[9] G. C. David, "Ergonomic methods for assessing exposure to risk factors for work-related musculoskeletal disorders," *Occupational Med.*, vol. 55, no. 3, pp. 190–199, May 2005.
[10] G. Li and P. Buckle, "Current techniques for assessing physical exposure to work-related musculoskeletal risks, with emphasis on posture-based methods," *Ergonomics*, vol. 42, no. 5, pp. 674–695, May 1999.
[11] L. McAtamney and E. N. Corlett, "RULA: A survey method for the investigation of work-related upper limb disorders," *Appl. Ergonom.*, vol. 24, no. 2, pp. 91–99, Apr. 1993.
[12] C. Wiktorin, M. Mortimer, L. Ekenvall, Å. Kilbom, and E. W. Hjelm, "HARBO, a simple computer-aided observation method for recording work postures," *Scandin. J. Work, Environ. Health*, vol. 21, no. 6, pp. 440–449, Dec. 1995.
[13] C. Fransson-Hall, R. Gloria, Å. Kilbom, J. Winkel, L. Karlqvist, and C. Wiktorin, "A portable ergonomic observation method (PEO) for computerized on-line recording of postures and manual handling," *Appl. Ergonom.*, vol. 26, no. 2, pp. 93–100, Apr. 1995.
[14] A. L. F. Rodacki and J. E. Vieira, "The effect of different supermarket checkout workstations on trunk kinematics of checkout operators," *Revista Brasileira de Fisioterapia*, vol. 14, no. 1, pp. 38–44, Feb. 2010.
[15] J. A. Diego-Mas and J. Alcaide-Marzal, "Using Kinect^{TM} sensor in observational methods for assessing postures at work," *Appl. Ergonom.*, vol. 45, no. 4, pp. 976–985, Jul. 2014.
[16] R. G. Radwin and M. L. Lin, "An analytical method for characterizing repetitive motion and postural stress using spectral analysis," *Ergonomics*, vol. 36, no. 4, pp. 379–389, Apr. 1993.
[17] W. S. Marras, F. A. Fathallah, R. J. Miller, S. W. Davis, and G. A. Mirka, "Accuracy of a three-dimensional lumbar motion monitor for recording dynamic trunk motion characteristics," *Int. J. Ind. Ergonom.*, vol. 9, no. 1, pp. 75–87, Jan. 1992.
[18] R. Alberto, F. Draicchio, T. Varrecchia, A. Silvetti, and S. Iavicoli, "Wearable monitoring devices for biomechanical risk assessment at work: Current status and future challenges—A systematic review," *Int. J. Environ. Res. Public Health*, vol. 15, no. 9, p. 2001, 2018.
[19] M. Nazarahari and H. Rouhani, "Semi-automatic sensor-to-body calibration of inertial sensors on lower limb using gait recording," *IEEE Sensors J.*, vol. 19, no. 24, pp. 12465–12474, Dec. 2019.
[20] M. Nazarahari, A. Noamani, N. Ahmadian, and H. Rouhani, "Sensor-to-body calibration procedure for clinical motion analysis of lower limb using magnetic and inertial measurement units," *J. Biomech.*, vol. 85, pp. 224–229, Mar. 2019, doi: 10.1016/j.jbiomech.2019.01.027.
[21] H. Rouhani, J. Favre, X. Crevoisier, and K. Aminian, "A wearable system for multi-segment foot kinetics measurement," *J. Biomech.*, vol. 47, no. 7, pp. 1704–1711, May 2014.
[22] M. Nazarahari and H. Rouhani, "Detection of daily postures and walking modalities using a single chest-mounted tri-axial accelerometer," *Med. Eng. Phys.*, vol. 57, pp. 75–81, Jul. 2018.
[23] A. Noamani, M. Nazarahari, J. Lewicke, A. H. Vette, and H. Rouhani, "Validity of using wearable inertial sensors for assessing the dynamics of standing balance," *Med. Eng. Phys.*, vol. 77, pp. 53–59, Mar. 2020.
[24] N. Ahmadian, M. Nazarahari, J. L. Whittaker, and H. Rouhani, "Quantification of triple single-leg hop test temporospatial parameters: A validated method using body-worn sensors for functional evaluation after knee injury," *Sensors*, vol. 20, no. 12, p. 3464, Jun. 2020.
[25] N. Vignais, M. Miezal, G. Bleser, K. Mura, D. Gorecky, and F. Marin, "Innovative system for real-time ergonomic feedback in industrial manufacturing," *Appl. Ergonom.*, vol. 44, no. 4, pp. 566–574, Jul. 2013.
[26] L. Peppoloni, A. Filippeschi, E. Ruffaldi, and C. A. Avizzano, "A novel wearable system for the online assessment of risk for biomechanical load in repetitive efforts," *Int. J. Ind. Ergonom.*, vol. 52, pp. 1–11, Mar. 2016.
[27] D. Battini, A. Persona, and F. Sgarbossa, "Innovative real-time system to integrate ergonomic evaluations into warehouse design and management," *Comput. Ind. Eng.*, vol. 77, pp. 1–10, Nov. 2014.
[28] E. S. Grood and W. J. Suntay, "A joint coordinate system for the clinical description of three-dimensional motions: Application to the knee," *J. Biomech. Eng.*, vol. 105, no. 2, pp. 136–144, May 1983.
[29] G. Wu, F. C. T. van der Helm, H. E. J. D. J. Veeger, M. Makhsous, P. Van Roy, C. Anglin, J. Nagels, A. R. Karduna, K. McQuade, X. Wang, F. W. Werner, and B. Buchholz, "ISB recommendation on definitions of joint coordinate systems of various joints for the reporting of human joint motion—Part II: Shoulder, elbow, wrist and hand," *J. Biomech.*, vol. 38, no. 5, pp. 981–992, May 2005.
[30] G. Wu, S. Siegler, P. Allard, C. Kirtley, A. Leardini, D. Rosenbaum, M. Whittle, D. D. D'Lima, L. Cristofolini, H. Witte, O. Schmid, and I. Stokes, "ISB recommendation on definitions of joint coordinate system of various joints for the reporting of human joint motion—Part I: Ankle, hip, and spine," *J. Biomech.*, vol. 35, no. 4, pp. 543–548, Apr. 2002.
[31] V. M. Manghisi, A. E. Uva, M. Fiorentino, V. Bevilacqua, G. F. Trotta, and G. Monno, "Real time RULA assessment using Kinect v2 sensor," *Appl. Ergonom.*, vol. 65, pp. 481–491, Nov. 2017.
[32] T. R. Water, V. Putz-Anderson, and A. Garg, "Applications manual for the revised NIOSH lifting equation," U.S Dept. Health Human Services, Public Health Services, Centers Disease Control Prevention, Nat. Inst. Occupat. Saf. Health, Division Biomed. Behav. Sci., Cincinnati, OH, USA, Tech. Rep. 94-110, 1994.

[33] P. Plantard, H. P. H. Shum, A.-S. Le Pierres, and F. Multon, "Validation of an ergonomic assessment method using Kinect data in real workplace conditions," *Appl. Ergonom.*, vol. 65, pp. 562–569, Nov. 2017.
[34] *Xsens MVN User Manual*, Xsens Technologies, Enschede, The Netherlands, 2019.
[35] J. R. Landis and G. G. Koch, "The measurement of observer agreement for categorical data," *Biometrics*, vol. 33, no. 1, pp. 159–174, 1977.
[36] K. O. McGraw and S. P. Wong, "Forming inferences about some intraclass correlation coefficients.," *Psychol. Methods*, vol. 1, no. 1, pp. 30–46, 2014.
[37] S. Qiu, Z. Wang, H. Zhao, and H. Hu, "Using distributed wearable sensors to measure and evaluate human lower limb motions," *IEEE Trans. Instrum. Meas.*, vol. 65, no. 4, pp. 939–950, Apr. 2016.
[38] A. R. Anwary, H. Yu, and M. Vassallo, "Optimal foot location for placing wearable IMU sensors and automatic feature extraction for gait analysis," *IEEE Sensors J.*, vol. 18, no. 6, pp. 2555–2567, Mar. 2018.
[39] F. Sun, W. Zang, R. Gravina, G. Fortino, and Y. Li, "Gait-based identification for elderly users in wearable healthcare systems," *Inf. Fusion*, vol. 53, pp. 134–144, Jan. 2020.
[40] B. M. Jolles, C. Duc, B. Coley, K. Aminian, C. Pichonnaz, J.-P. Bassin, and A. Farron, "Objective evaluation of shoulder function using body-fixed sensors: A new way to detect early treatment failures?" *J. Shoulder Elbow Surgery*, vol. 20, no. 7, pp. 1074–1081, Oct. 2011.
[41] C. Pichonnaz, C. Duc, B. M. Jolles, K. Aminian, J.-P. Bassin, and A. Farron, "Alteration and recovery of arm usage in daily activities after rotator cuff surgery," *J. Shoulder Elbow Surgery*, vol. 24, no. 9, pp. 1346–1352, Sep. 2015.
[42] L. Peppoloni, A. Filippeschi, and E. Ruffaldi, "Assessment of task ergonomics with an upper limb wearable device," in *Proc. 22nd Medit. Conf. Control Autom.*, Jun. 2014, pp. 340–345.
[43] X. Robert-Lachaine, H. Mecheri, C. Larue, and A. Plamondon, "Validation of inertial measurement units with an optoelectronic system for whole-body motion analysis," *Med. Biol. Eng. Comput.*, vol. 55, no. 4, pp. 609–619, Apr. 2017.
[44] A. Filippeschi, N. Schmitz, M. Miezal, G. Bleser, E. Ruffaldi, and D. Stricker, "Survey of motion tracking methods based on inertial sensors: A focus on upper limb human motion," *Sensors*, vol. 17, no. 6, p. 1257, Jun. 2017.
[45] M. Nazarahari and H. Rouhani, "40 years of sensor fusion for orientation tracking via magnetic and inertial measurement units: Methods, lessons learned, and future challenges," *Inf. Fusion*, vol. 68, pp. 67–84, Apr. 2021.
[46] G. Ligorio, D. Zanotto, A. M. Sabatini, and S. K. Agrawal, "A novel functional calibration method for real-time elbow joint angles estimation with magnetic-inertial sensors," *J. Biomech.*, vol. 54, pp. 106–110, Mar. 2017.
[47] P. Picerno, P. Caliandro, C. Iacovelli, C. Simbolotti, M. Crabolu, D. Pani, G. Vannozzi, G. Reale, P. M. Rossini, L. Padua, and A. Cereatti, "Upper limb joint kinematics using wearable magnetic and inertial measurement units: An anatomical calibration procedure based on bony landmark identification," *Sci. Rep.*, vol. 9, no. 1, pp. 1–10, Dec. 2019.
[48] E. Palermo, S. Rossi, F. Marini, F. Patanè, and P. Cappa, "Experimental evaluation of accuracy and repeatability of a novel body-to-sensor calibration procedure for inertial sensor-based gait analysis," *Measurement*, vol. 52, no. 1, pp. 145–155, Jun. 2014.
[49] M. A. Soriano, F. Khan, and R. Ahmad, "Two-axis accelerometer calibration and nonlinear correction using neural networks: Design, optimization, and experimental evaluation," *IEEE Trans. Instrum. Meas.*, vol. 69, no. 9, pp. 6787–6794, Sep. 2020.
[50] V. Renaudin, M. H. Afzal, and G. Lachapelle, "New method for magnetometers based orientation estimation," in *Proc. IEEE/ION Position, Location Navigat. Symp.*, May 2010, pp. 348–356.

AHMED HUMADI was born in Hadhramout, Yemen, in 1991. He received the B.Sc. degree in mechanical engineering from King Saud University, Riyadh, Saudi Arabia, in 2016, and the M.Sc. degree in mechanical engineering from the University of Alberta, Edmonton, AB, Canada, in 2020. From 2018 to 2020, he worked on the work-related musculoskeletal injuries assessment. His research interests include video-based and wearable technologies in human motion biomechanics.

MILAD NAZARAHARI was born in Tehran, Iran, in 1988. He received B.Sc. and M.Sc. degrees in mechanical engineering from the Iran University of Science and Technology, Tehran, in 2012 and 2014, respectively. He is currently pursuing the Ph.D. degree with the Mechanical Engineering Department, University of Alberta, Edmonton, AB, Canada. From 2012 to 2016, he was a Research Assistant with the Iran University of Science and Technology, working on the application of artificial intelligence in biomedical signal classification. Since September 2016, he has been a Research and Teaching Assistant with the Mechanical Engineering Department, University of Alberta. His research interests include wearable technology in human motion biomechanics, biomedical and rehabilitation engineering, applications of artificial intelligence, and control theory in biomedical engineering and signal processing. He is also a member of the International Society of Biomechanics and the European Society of Biomechanics.

RAFIQ AHMAD received the B.Sc. degree in mechanical engineering from the University of Engineering and Technology Peshawar, Pakistan, and the master's degree in design and manufacturing from the Ecole Nationale Superieure d'Arts et Metiers (ENSAM-Paris), France. He is currently pursuing the Ph.D. degree in advanced manufacturing with the Ecole Centrale de Nantes, France. He is also an Assistant Professor with the Department of Mechanical Engineering, University of Alberta. He is also the Founder and Director of the Laboratory of Intelligent Manufacturing, Design and Automation (LIMDA), focusing on "hybrid and smart systems." His research interests include smart systems design and development for Industry 4.0, hybrid-manufacturing combining additive and subtractive technologies, repair and remanufacturing, sensor and the IoT technologies, and industrial automation and robotics. He received the Postdoctoral Fellow for a two-year from the University of Luxembourg. He is running numerous research programs and industrial collaborations targeting the implementation of Industry 4.0, smart manufacturing, and green technologies. He is also a Board Member of the International Society of Automation (ISA-Edmonton Section, a Co-UofA Student Section Advisor) and a member of APEGA and ASME. He is also an active editor, a reviewer, and an organizer of numerous international conferences and journals.

HOSSEIN ROUHANI (Member, IEEE) received the B.Sc. degree in mechanical engineering from the Amirkabir University of Technology, the M.Sc. degree in mechanical engineering from the University of Tehran, Iran, and the Ph.D. degree in biotechnology and bioengineering from the Swiss Federal Institute of Technology in Lausanne (EPFL), in 2010. He was a Postdoctoral Fellow with EPFL in 2011. He was then a Postdoctoral Fellow with the Institute of Biomaterials and Biomedical Engineering, University of Toronto, from 2012 to 2015. He has been an Assistant Professor with the Department of Mechanical Engineering, University of Alberta, and a Research Affiliate of the Glenrose Rehabilitation Hospital (Edmonton) since 2015. His research interests include musculoskeletal biomechanics, biomedical instrumentation design, and the development of wearable neuro-rehabilitative technologies. He was a recipient of two postdoctoral fellowship awards from the Swiss National Science Foundation and an Associate Editor in the *Canadian Journal of Electrical and Computer Engineering* and *Frontiers in Sports and Active Living*.